IEEE Access
Multidisciplinary ⋮ Rapid Review ⋮ Open Access Journal

Received January 23, 2021, accepted May 5, 2021, date of publication May 11, 2021, date of current version May 28, 2021.

Digital Object Identifier 10.1109/ACCESS.2021.3079274

The Impact of Control Point Dispersion on Measurement Accuracy in a New Type of Light-Pen Coordinate Measuring System

DONGRI SHAN[1], XIAODONG BI[2], XIAOFANG WANG[1], PENG ZHANG[1], ZHOUFANG XU[1], MIN HAN[1], YANG LIU[3], CHENGLONG ZHANG[2], AND YALU XU[2]

[1]School of Electronic and Information Engineering, Qilu University of Technology (Shandong Academy of Sciences), Jinan 250300, China
[2]School of Mechanical and Automotive Engineering, Qilu University of Technology (Shandong Academy of Sciences), Jinan 250300, China
[3]College of Instrumentation and Electrical Engineering, Jilin University, Changchun 130061, China

Corresponding author: Dongri Shan (shandongri@qlu.edu.cn)

This work was supported in part by the Project of Shandong Province Major Science and Technology Innovation under Grant 2019JZZY010444 and Grant 2019TSLH0315, in part by the Project of Jinan 20 Policies to Support Development of University under Grant 2019GXRC063, in part by the Project of Shandong Province Higher Educational Science and Technology Program under Grant J18KA345, and in part by the Natural Science Foundation of Shandong Province of China under Grant ZR2020MF138.

ABSTRACT Light-pen coordinate measuring machines are widely used due to their portability; however, the measurement accuracy is affected by camera calibration, light-pen probe calibration, control points, etc. To study the influence of control point dispersion on measurement accuracy, a light-pen coordinate measuring system is constructed in this paper. In this system, a new type of control point distribution is designed. Based on this distribution, five light-pens with different control point dispersions are created and an algorithm is proposed to match control points with their images. The experimental repeatability results for the five light-pen probes indicate satisfactory repeatability, which ensures the effectiveness of the measurement results. The experimental measurement results for five light-pens demonstrate that the measurement error decreases with the decline of the control point dispersion at first, but begins to increase when the control point dispersion reaches a certain value.

INDEX TERMS Light-pen coordinate measuring system, light-pen, control point distribution, control point dispersion, measurement accuracy.

I. INTRODUCTION

With the continuous progress in manufacturing and continuously increasing industrial measurement requirements, one-dimensional and two-dimensional measurement methods cannot meet the needs of industrial technology development. The first coordinate measuring machine (CMM) was successfully developed by the Ferranti company (UK) in 1960 [1]. A CMM offers high measurement accuracy and versatility and is important in industrial product inspection. However, the large size of traditional frame-type CMMs is inconvenient for on-site measurement and limits the monitoring range. Thus, articulated-arm CMMs, laser trackers, indoor GPS, mobile space coordinate measuring machines, photogrammetric systems, and other new portable coordinate measuring machines (PCMMs) that are convenient for on-site and large-scale measurement tasks have been widely developed [2]–[6].

Recent research has focused on fast and portable measurements of large parts. The portable coordinate measuring machines (PCMMs) can conveniently complete rapid on-site measurement tasks and have been widely used in large-scale engineering metrology. The light-pen coordinate measuring machines (LPCMMs) are small, light, convenient, highly accurate, and produce no interference light. They are suitable for on-site measurements and are widely used for the measurement of large parts [7]. Vision-based LPCMMs have become the main research focus in the measurement field. There are two types of measurement techniques: noncontact and contact. Typical noncontact PCMMs include laser and white light scanners [8], laser tracking systems, and charge-coupled device (CCD) cameras [9]–[11].

The associate editor coordinating the review of this manuscript and approving it for publication was Wuliang Yin.

Light-pen measurement technology has developed rapidly since the 1990s. Many light-pen measuring products, including the V-ATARS system from GSI (US) [12], the Tritop system from Gom (Germany), the ATOS contact probe system, the DUO and SOLO systems from Metronor (Norway) [13], and the HandyProbe (NEXT) system (Canada) [14], are commercially available. In 2005, Liu and Huang first proposed a single-camera light-pen vision measuring system. They studied a mathematical model of a single-camera light-pen vision system and its solutions, which improved the stability of the measurement [15]. Many researchers have subsequently studied light-pen PCMMs for monocular and binocular vision measurements [16]–[20].

The light-pen calibration accuracy, camera calibration accuracy [21], and control points on the light-pen can affect the measurement accuracy of the light-pen coordinate measuring system. Control points directly monitor objects in a vision measuring system; their number and geometric distribution structure can affect the measurement accuracy. Through simulation experiments, Jiang found that when the image positioning accuracy was constant and the number of control points increased from four to eight, the accuracy of attitude measurement was significantly improved. However, when the number of control points exceeded eight, the growth rate of accuracy decreased [22]. Targeting the linear distribution, cross distribution, circular distribution, and planar matrix distribution of control points, Weng conducted simulation experiments and found that when the control point distribution is a rectangular layout, the measurement accuracy is the highest [23]. However, there is little research on the influence of control points on measurement accuracy; nevertheless, the influence on measurement accuracy is real. At present, only the number and distribution of control points have been studied, whereas control point dispersion has not been studied. Huang used a three-point linear light-pen to study the distance between control points [24]; however, the number of control points was too small to provide strong evidence for this research.

To further explore the influence of control point dispersion on measurement accuracy, a light-pen coordinate measuring system is constructed, and repeatability experiments and measurement experiments are performed in this paper. To be specifically, the contributions are five-fold: 1) a control point distribution is designed, based on which, five light-pens with different dispersions are constructed; 2) an algorithm matching the control points and their images is proposed; 3) repeatability experiments and measurement experiments are performed to verify the stability of the measuring system and reveal the relationship between control point dispersion and measurement accuracy.

The remainder of this paper is organized as follows. The light-pen coordinate measuring system is introduced in Section II. Theoretical analysis for the influence of control point dispersion on measurement accuracy is introduced in Section III. Repeatability experiments and measurement experiments are conducted in Section IV.

II. LIGHT-PEN COORDINATE MEASURING SYSTEM

As depicted in Fig. 1, the LPCMM comprises three parts: 1) a CCD camera; 2) a computer; 3) a light-pen. During measurement, the operator touches the workpiece with the light-pen probe. Images are captured and transmitted to the computer. The computer processes the images and calculates the measurement result using a program.

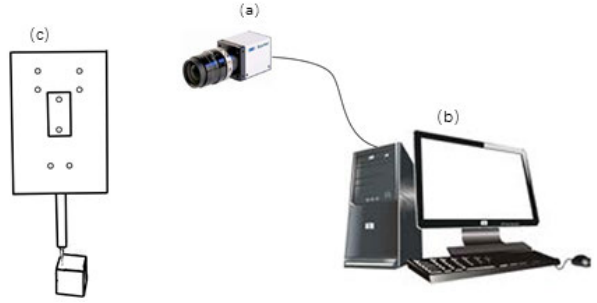

FIGURE 1. System diagram.

A. COORDINATE SYSTEM ESTABLISHMENT

As depicted in Fig. 2, the measuring system model includes three coordinate systems:

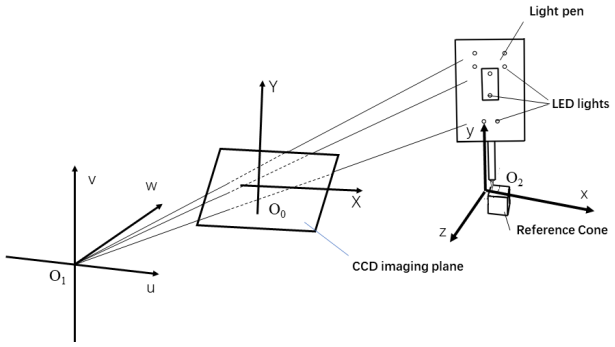

FIGURE 2. Coordinate system.

1) IMAGE COORDINATE SYSTEM($O_0 - XY$)

The coordinate system is established on the image plane of the camera; the centre of the image plane is the origin of the coordinate O_0. The x-axis and y-axis are parallel to the horizontal and vertical scanning directions of the CCD camera, respectively, and should be parallel to the O_1-uv plane. (unit: pixel)

2) CAMERA COORDINATE SYSTEM ($O_1 - uvw$)

The origin of the coordinate system O_1 is the optical centre of the camera. The w-axis is the optical axis, and the u- and v-axes are respectively parallel to the horizontal and vertical axes of the image coordinate system. (unit: mm)

3) LIGHT-PEN COORDINATE SYSTEM ($O_2 - xyz$)

The origin of the coordinate system O_2 is established on the light-pen probe. The connection direction of control points 3 and 6 is the x-axis direction (the coding of control

points is depicted in Fig. 4). The connection direction of control points 1 and 2 is the y-axis direction. The O_2–xy plane is perpendicular to the z-axis. (unit: mm)

B. CONTROL POINT DISTRIBUTION AND LIGHT-PEN DESIGN

As depicted in Fig. 3, the light-pen body is equipped with eight infrared LED light points and a detachable ruby spherical probe (shape error is less than 0.1%). The control points of the light-pen are represented by an infrared LED lamp whose wavelength is greater than that of visible light. A filter of the corresponding wavelength is placed in front of the lens to effectively capture the control points, optimise the shooting environment, reduce the image processing steps, accelerate the processing efficiency, and improve the measurement accuracy.

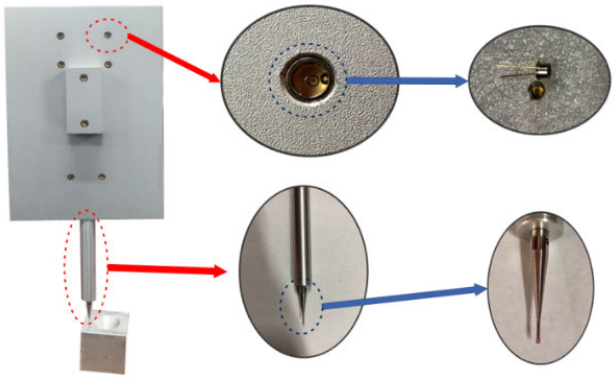

FIGURE 3. Structure of light-pen.

The research in recent years have shown that when the number of control points exceeded eight, the growth rate of accuracy decreases. Increasing the number of control points increases the calculations. Therefore, eight control points are selected. The distribution of the control points also affects the measurement accuracy. When the distribution is linear or rectangular, the measurement accuracy is higher than that with other distributions. A new type of control point distribution is designed (Fig. 3). The eight control points arranged into a rectangular and linear distribution. Making the middle two control points higher than the other control points, improves the measurement accuracy of the LPCMM in the direction of the camera's optical axis.

Based on the control point distribution, five light-pens with different control point dispersions are designed with the premise that the number and structure distribution remain unchanged. The distances between the eight control points for the five light-pens are as follows:

Light-Pen A: The distance between control points 3, 4, 6, 7 and the centre line is 35 mm (the coding of the control points is shown in Fig. 4.); the distance between control points 3 and 4 in the x-axis direction is 40 mm; the distance between control points 6 and 7 in the x-axis direction is 40 mm; the distance between points 5, 8 and the centre line is 20 mm.

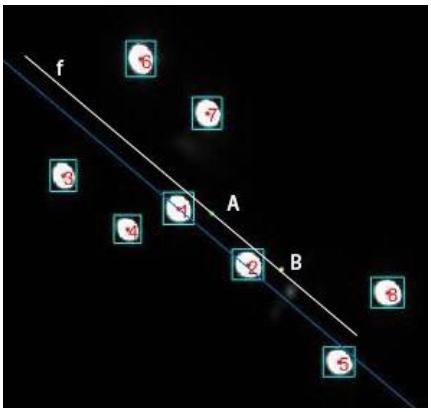

FIGURE 4. Matching control points and their images.

Light-Pen B: The distance between control points 3, 4, 6, 7 and the centre line is 30 mm; the distance between control points 3 and 4 in the x-axis direction is 35 mm; the distance between control points 6 and 7 in the x-axis direction is 35 mm; the distance between points 5, 8 and the centre line is 18 mm.

Light-Pen C: The distance between control points 3, 4, 6, 7 and the centre line is 25 mm; the distance between control points 3 and 4 in the x-axis direction is 30 mm; the distance between control points 6 and 7 in the x-axis direction is 30 mm; the distance between points 5, 8 and the centre line is 15 mm.

Light-Pen D: The distance between control points 3, 4, 6, 7 and the centre line is 20 mm; the distance between control points 3 and 4 in the x-axis direction is 25 mm; the distance between control points 6 and 7 in the x-axis direction is 25 mm; the distance between points 5, 8 and the centre line is 12 mm.

Light-Pen E: The distance between control points 3, 4, 6, 7 and the centre line is 15 mm; the distance between control points 3 and 4 in the x-axis direction is 20 mm; the distance between control points 6 and 7 in the x-axis direction is 20 mm; the distance between points 5, 8 and the centre line is 10 mm.

Control point dispersion is defined by the standard deviation of the coordinates of all control points on the x-, y-, and z-axes. The centre coordinates of the control points and the light-pen probe in the light-pen coordinate system are obtained by the light-pen calibration. The light-pen is calibrated by a high-precision coordinate measuring machine made in the UK. The Maximum Permissible Error (MPE) of the high-precision coordinate measuring machine changes with the measurement distance L (the distance between the camera and the measured object): $MPE = 5.0 + L/330$. The unit of MPE is micron and the unit of L is millimetre.

To simplify the calculation, we set the centre of the light-pen probe as the origin of the light-pen coordinate system. The calibration results of control points are shown in TABLE 1. It can be seen from the last column that the

TABLE 1. Calibration results of five light-pen control points.

(mm)

		1	2	3	4	5	6	7	8	Std
A	x	-160.369	-130.359	-220.351	-180.345	-90.323	-220.355	-180.342	-90.334	48.338
	y	0.182	0.190	-34.829	-34.830	-19.816	35.176	35.181	20.185	26.695
	z	26.065	26.065	6.236	6.236	6.236	6.236	6.236	6.236	8.586
B	x	-165.126	-135.136	-218.095	-183.097	-95.080	-218.094	-183.089	-95.078	45.921
	y	-0.065	-0.060	-30.052	-30.058	-17.945	29.955	29.953	17.945	23.036
	z	26.366	26.366	6.446	6.446	6.446	6.446	6.446	6.446	8.625
C	x	-170.350	-140.263	-215.371	-185.782	-100.199	-215.383	-185.510	-100.298	43.226
	y	1.131	0.879	-23.947	-24.067	-14.053	26.333	26.199	15.922	19.289
	z	24.817	24.817	4.714	4.714	4.714	4.714	4.714	4.714	8.705
D	x	-175.075	-145.073	-212.069	-187.064	-105.046	-212.064	-187.057	-105.042	40.439
	y	-0.414	-0.415	-20.401	-20.407	-11.657	19.603	19.602	10.852	15.223
	z	26.797	26.797	6.834	6.834	6.834	6.834	6.834	6.834	8.644
E	x	-180.309	-150.307	-210.314	-190.312	-110.302	-210.314	-190.313	-110.302	38.226
	y	-0.498	-0.495	-15.488	-15.491	-10.488	14.511	14.513	9.512	11.726
	z	25.876	25.876	5.988	5.988	5.988	5.988	5.988	5.988	8.611

control point dispersion from light pen A to light pen E gradually decreases.

C. MATCHING CONTROL POINTS AND IMAGES

In the light-pen measuring system, the one-to-one correspondence between the control points and their images is significance. An algorithm is designed that can quickly and accurately match the control points and their images. The algorithm significantly improves the calculation speed, further improving the measurement speed of the system, which is beneficial for industrial measurement.

Camera imaging is a perspective projection process from a three-dimensional object space to a two-dimensional image plane. For objects with the same shape in a three-dimensional space, when the camera is positioned at a different angle, the shape in the obtained two-dimensional image is different. Thus, a shape description method that is not affected by perspective projection must be adopted [25].

In perspective projection, there exists a linear relationship between the coordinate u_i of the object in the camera coordinate system and the coordinate X_i of the object in the image coordinate system; $X_i = \alpha u_i$, where α is the coefficient of linear transformation. It is observed that the image formed by the perspective projection of a straight line in space is still a straight line, and the projection of a straight line $f = ax + by + c$ is $f' = a'x + b'y + c'$.

$$\left.\begin{array}{c} \forall (x, y) \in f \rightarrow (ax, ay) \in f', a \neq 0 \\ f = ax + by + c \rightarrow f = \frac{a}{\alpha}(\alpha x) + \frac{b}{\alpha}(\alpha y) + c \end{array}\right\} \rightarrow f' = \frac{a}{\alpha}x + \frac{b}{\alpha}y + c. \quad (1)$$

As depicted in Fig. 4, the control points of the light-pen are sorted.

The process of matching control points and their images is described as follows:

1. The computer processes the images to obtain the centre coordinates of the control points in the image coordinate system, $p_i = (x_i, y_i)$, $i \in [1, 8]$.

2. Using principal component analysis to perform straight-line fitting of the centre coordinates of light-pen control points, the centre line f is obtained, and the centre point of all the control point is point A.

3. The control point that is closest to the centre point A is point 1.

4. The control point that meets the following two constraints is point 2: i) The distance between the control point and the centre point A is the shortest, $\min(d_{iA})$, $i = \in [1, 8]$. ii) The distance between the control point and point 1 is the shortest, $\min(d_{i1})$, $i = \in [2, 8]$.

5. Owing to the offset during the light-pen measurement process, the connection line between points 1 and 2 is not a symmetrical line of the other control points. The centre point A of the light-pen is calculated; thus, the displacement vector between point 1 and centre point A can be obtained. The position of point B is found through point 2 and the same displacement vector.

6. The unnamed control points are connected to points A and B; the connected straight lines are l_{iA} and l_{iB}. The rotation direction from l_{iA} to l_{iB} is compared using the top and bottom of l_{iA} and l_{iB}. The direction of rotation is clockwise at points 3, 4, and 5 (l_{iA} is higher than l_{iB}), and the direction of rotation is clockwise at points 6, 7, and 8 (l_{iA} is lower

than l_{iB}). Each point is determined by its y-axis coordinate.

D. MODEL COORDINATE SYSTEM CONVERSION SOLUTION

Assuming that the centre coordinates of the eight control points in the light-pen coordinate system are (x_j, y_j, z_j), those in the image coordinate system are $(X_j, Y_j,)$, and those in the camera coordinate system are (u_j, v_j, w_j), $j = 1, 2, 3 \cdots 8$, the transformation from the light-pen coordinate system to the camera coordinate system can be expressed as:

$$\begin{bmatrix} u \\ v \\ w \end{bmatrix} = \begin{bmatrix} R & T \end{bmatrix} \begin{bmatrix} x \\ y \\ z \\ 1 \end{bmatrix} = \begin{bmatrix} r_1 & r_2 & r_3 & t_x \\ r_4 & r_5 & r_6 & t_y \\ r_7 & r_8 & r_9 & t_z \end{bmatrix} \begin{bmatrix} x \\ y \\ z \\ 1 \end{bmatrix} \quad (2)$$

where $R = \begin{bmatrix} r_1 & r_2 & r_3 \\ r_4 & r_5 & r_6 \\ r_7 & r_8 & r_9 \end{bmatrix}$, $T = \begin{bmatrix} t_x \\ t_y \\ t_z \end{bmatrix}$

The centre coordinate of the light-pen probe in the camera coordinate system can be obtained using Equation (2). R is the rotation orthogonal matrix, and T is the translation matrix.

Before measurement, the CCD camera is pre-calibrated [26]. During measurement, the images of the light-pen and eight LED control points are captured by the CCD camera. The captured images are transmitted to the computer via a gigabit network cable. The software installed on the computer processes the images to obtain centre coordinates of the control points in the image coordinate system.

There exists a projection relationship between the camera coordinate system and the image coordinate system. The centre coordinates in the camera coordinate system can be calculated by substituting the image centre coordinates into Equation (3).

$$s_j \cdot \begin{bmatrix} X_j \\ Y_j \\ 1 \end{bmatrix} = \begin{bmatrix} f & 0 & 0 \\ 0 & f & 0 \\ 0 & 0 & f \end{bmatrix} \begin{bmatrix} u_j \\ v_j \\ w_j \end{bmatrix} \quad (3)$$

The scale factor for the conversion between the camera coordinate system and the image coordinate system is s_j. The focal length of the camera lens is f. According to the perspective projection, Equations (2) and (3) can be combined to obtain:

$$\begin{aligned} s_{\mathrm{j}} \cdot \begin{bmatrix} X_j \\ Y_j \\ 1 \end{bmatrix} &= \begin{bmatrix} f & 0 & 0 \\ 0 & f & 0 \\ 0 & 0 & f \end{bmatrix} \begin{bmatrix} r_{1i} & r_{2i} & r_{3i} & t_{xi} \\ r_{4i} & r_{5i} & r_{6i} & t_{yi} \\ r_{7i} & r_{8i} & r_{9i} & t_{zi} \end{bmatrix} \begin{bmatrix} x_j \\ y_j \\ z_j \\ 1 \end{bmatrix} \\ &= \begin{bmatrix} fr_{1i} & fr_{2i} & fr_{3i} & ft_{xi} \\ fr_{4i} & fr_{5i} & fr_{6i} & ft_{yi} \\ r_{7i} & r_{8i} & r_{9i} & t_{zi} \end{bmatrix} \begin{bmatrix} x_j \\ y_j \\ z_j \\ 1 \end{bmatrix} \end{aligned} \quad (4)$$

The initial values of R and T are obtained using the centre coordinates in the light-pen coordinate system of the eight control points and corresponding image centre coordinates [27].

According to Equation (4), the following equation is obtained:

$$\begin{cases} f_{aj} = f\left(r_1 x_j + r_2 y_j + r_3 z_j + t_x\right) \\ \qquad\qquad -X_j\left(r_7 x_j + r_8 y_j + r_9 z_j + t_z\right) = 0 \\ f_{bj} = f\left(r_4 x_j + r_5 y_j + r_6 z_j + t_y\right) \\ \qquad\qquad -Y_j\left(r_7 x_j + r_8 y_j + r_9 z_j + t_z\right) = 0 \end{cases}$$
$$j = 1, 2 \cdots N \quad (5)$$

The objective function that minimises the sum of squares of the spatial coordinate errors can be expressed as

$$I\left(r_1, r_2 \cdots r_9, t_x, t_y, t_z\right) = \sum_{j=1}^{n} \left(f_{aj}^2 + f_{bj}^2\right) = \min \quad (6)$$

The optimal solution is obtained by the objective function, which yields the R and T of the image.

After the rotation matrix R and the translation vector T are obtained using the nonlinear least square generalised inverse method given in [28]. The centre coordinate of probe in the light-pen coordinate system, R and T are substituted into Equation (2) to obtain the centre coordinate of the light-pen probe in the camera coordinate system.

E. MEASUREMENT METHOD

The key to performing measurement using a light-pen coordinate measuring system is to obtain the centre coordinate of the light-pen probe in the camera coordinate system, which are performed by following steps:

1. During measurement, the light-pen probe is placed in the measured object by the operator. Control points are captured by the CCD camera with a filter and the images are transmitted to the computer in real time.

2. The centre coordinates of each light-pen control points in the image coordinate system are obtained through Least Squares Fitting of Ellipse of image processing.

3. The rotation matrix R and translation vector T of the conversion between the camera coordinate system and the light-pen coordinate system are obtained using the calibrated centre coordinates of the eight control points in the light-pen coordinate system and corresponding image centre coordinates based on Equation (4)(5)(6).

4. The calibrated centre coordinate of the light-pen probe in the light-pen coordinate system and R and T are substituted into Equation (2) to obtain the centre coordinate of the light-pen probe in the camera coordinate system.

III. INFLUENCE OF CONTROL POINT DISPERSION ON MEASUREMENT ACCURACY

Fig. 5 depicts a light-pen with three control points [24]. The size of the light-pen body includes the positioning dimensions L_1, L_2, and L_3 between the centres of the three control points, the positioning dimension L_4 between the lowest control point and the probe, and the total length of the light-pen L_0. The values of L_0, L_1, L_2, L_3, and L_4 are determined according to the focal length and angle of view of the selected

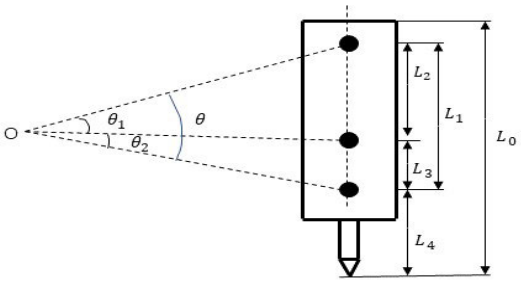

FIGURE 5. Schematic of three-point light-pen.

CCD camera lens and the field of view H. As depicted in Fig. 6, $H = Lh/f$; after selecting the camera and lens, H and f can be determined. Thus, if L is known, H can be determined.

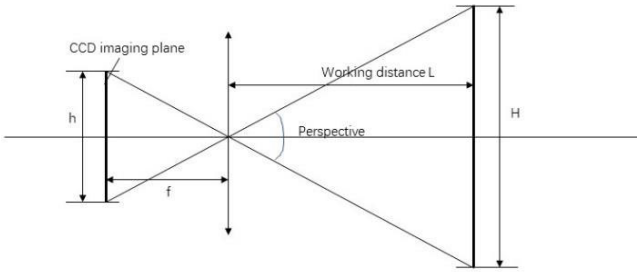

FIGURE 6. Camera field of view range.

According to the determined camera field of view range H and the light-pen structure, the centre distance L_1 between the upper and lower control points can be determined. The parameters $\theta_1, \theta_2, \theta = \theta_1 + \theta_2$ (Fig. 5) are obtained from the image centre coordinates of the corresponding control points to solve the collinear three-point perspective problem (P3CP) [29]. Under the premise that the extraction accuracy of the image plane of the control points is certain (pixel or subpixel level), the relative error of the calculated value of θ decreases when the value of θ increases, the P3CP solution accuracy increases, and the measurement accuracy increases. Thus, the distance between the control points theoretically affects the measurement accuracy.

After the centre coordinates of the three control points in the camera coordinate system are obtained, the centre coordinate of the probe can be solved using any two control points collinear with the centre of the probe to obtain three sets of coordinates, and the average value can be calculated.

From the geometric relationship depicted in Fig. 7, L' is the centre distance between the highest control point and the probe centre, and L_1 is the centre distance between the highest and lowest control points. Assuming that the centre distance L_2 of the upper two control points and the centre distance L' remain unchanged, the centre distance increases from L_1 to L_1', assuming that there is no positioning error in the upper two control points, and the positioning error of the bottom control point is Δ. As depicted in Fig. 7, the presence

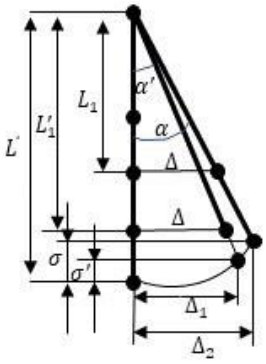

FIGURE 7. Positioning error of control points.

of Δ produces errors in the calculated pen tip position in both the horizontal and vertical directions. Δ_1 and Δ_2 are the errors in the horizontal direction, σ and σ' are the errors in the vertical direction.

$$\begin{aligned} \Delta_2 &= \mathrm{L}'\sin\alpha \approx L'\frac{\Delta}{L_1} \\ \Delta_1 &= L'\sin\alpha' \approx L'\frac{\Delta}{L_1'} \\ \sigma &= L'(1-\cos\alpha) \\ \sigma' &= L'\left(1-\cos\alpha'\right) \end{aligned} \tag{7}$$

According to Equation (7), because $L_1' > L_1, \alpha' < \alpha$ and $\Delta_1 < \Delta_2, \sigma' < \sigma$. It can be seen that the distance between the control points affects the measurement accuracy.

IV. EXPERIMENTS

To demonstrate the effectiveness of the measurement experiment, a repeatability experiment is conducted first. A measurement experiment is conducted to study the influence of dispersion on measurement accuracy.

A. REPEATABILITY EXPERIMENT

As depicted in Fig. 8, a standard cone is fixed on the measuring table, and the light-pen probe is placed in the reference cone. Under the premise of ensuring that the light-pen probe does not leave the lowest end of the reference cone, the operator rotates the position of the light-pen and captures an image at each position. In total, ten images are captured for each light-pen. The centre coordinate of the light-pen probe in the

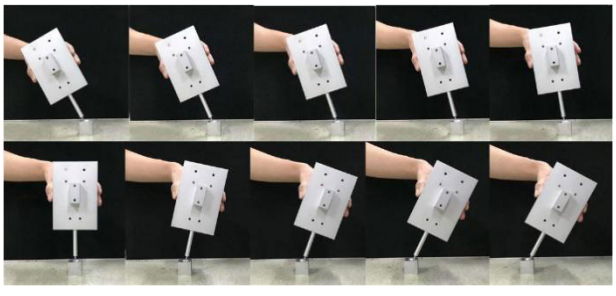

FIGURE 8. Repeatability experiment.

TABLE 2. Centre coordinates of five light-pen probes.

(mm)

	NO.	1	2	3	4	5	6	7	8	9	10	Std
A	u	25.473	25.509	25.511	25.487	25.512	25.472	25.481	25.481	25.524	25.510	0.019
	v	107.513	107.508	107.543	107.506	107.549	107.533	107.578	107.578	107.542	107.475	0.033
	w	1034.508	1034.424	1034.381	1034.546	1034.501	1034.501	1034.455	1034.455	1034.411	1034.538	0.056
B	u	24.390	24.430	24.448	24.463	24.423	24.452	24.464	24.443	24.486	24.413	0.028
	v	107.520	107.535	107.476	107.451	107.412	107.457	107.517	107.507	107.432	107.342	0.060
	w	1023.327	1023.388	1023.303	1023.382	1023.340	1023.326	1023.302	1023.349	1023.448	1023.455	0.055
C	u	24.685	24.664	24.667	24.681	24.669	24.687	24.710	24.705	24.674	24.701	0.016
	v	107.990	107.978	107.998	108.001	107.979	108.025	107.976	108.017	108.022	107.961	0.022
	w	1029.975	1029.957	1029.865	1029.806	1030.025	1029.920	1030.073	1030.036	1029.995	1029.922	0.082
D	u	24.975	24.979	24.943	24.999	24.974	24.931	24.981	24.961	25.015	24.958	0.025
	v	107.575	107.582	107.556	107.527	107.492	107.498	107.649	107.631	107.576	107.535	0.052
	w	1023.018	1023.036	1023.124	1023.034	1022.950	1022.936	1023.071	1023.089	1023.083	1022.903	0.073
E	u	24.446	24.448	24.553	24.464	24.477	24.461	24.436	24.439	24.419	24.382	0.044
	v	105.725	105.865	105.787	105.957	105.963	105.911	105.902	105.857	105.868	105.914	0.074
	w	1034.998	1034.974	1035.005	1035.142	1034.965	1035.017	1035.036	1035.060	1035.036	1034.967	0.053

camera coordinate system in the 10 images obtained by the measurement method in Subsection E of Section II.

The experimental results for the five light-pens are presented in TABLE 2. The centre point coordinates of each light-pen probe in the ten images are shown in the columns numbered by 1 to 10. The repeatability is represented by the standard deviation of ten centre point coordinates. As presented in the last column, the probe repeatability of each light-pen does not exceed 0.082, and its convergence speed is satisfactory.

B. MEASUREMENT EXPERIMENT

As depicted in Fig. 9(a), the measurement object is a reference cone. The reference width of the cone is 30.0317 mm, which is obtained by a high-precision coordinate measuring machine.

The width of the reference cone is measured using the new light-pen measuring system by following steps: 1) the operator captures images from the left and right sides of the reference cone. As depicted in Fig. 9(b), for each light-pen, the operator touches 15 different positions on the left surface of the reference cone to capture 15 images. This operation is repeated on the right surface, as depicted in Fig. 9(c); 2) the captured images are transferred to a computer. The coordinate position results of light-pen probe in the camera coordinate system obtained by the measurement method in Subsection E of Section II; 3) as depicted in Fig. 10, the points on the right surface are fitted to a plane by singular value decomposition (SVD) [30]. The measured width is obtained by calculating the average distance from the points on the left surface to the fitted plane on the right.

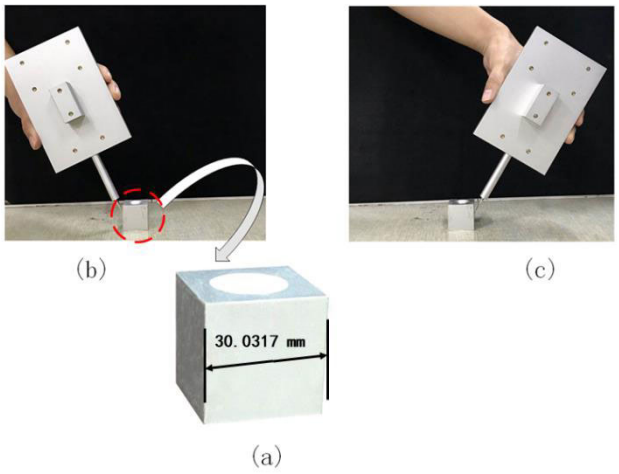

FIGURE 9. Image acquisition.

Ten measurement experiments are performed for each light-pen. The measurement results are presented in TABLE 3. The measured widths of five light-pens are shown in rows 2–11. The average value, absolute error, and relative error are shown in the last three rows.

TABLE 3 shows that the measured average values of the five light-pens are not the same. The closest to the reference value of 30.0317 mm is obtained by light-pen C. The measured average value is 30.1237 mm, the absolute error is 0.092 mm, and the relative error is 0.31%. The errors of the remaining four light-pens are all higher than those of light-pen C.

From the control point dispersion of five light-pens in TABLE 1 and the absolute error and relative error of the

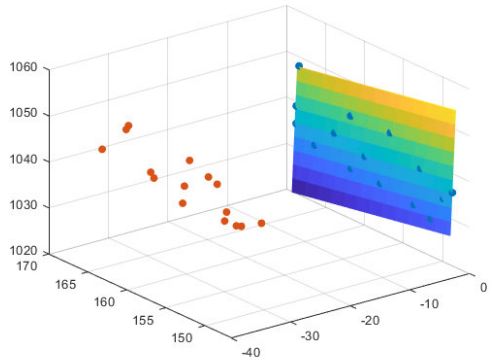

FIGURE 10. Results of centre point of light-pen probe in the camera coordinate system.

TABLE 3. Measurement results of five light-pens.

(mm)

Light-pen / No.	A	B	C	D	E
1	30.656	29.942	29.997	30.410	29.694
2	30.698	30.580	30.235	30.376	30.160
3	30.318	30.358	30.101	30.451	30.208
4	30.654	30.662	30.125	30.046	30.564
5	30.518	30.410	30.245	30.164	30.414
6	30.500	30.263	30.274	30.332	30.476
7	30.431	30.358	30.163	30.157	30.429
8	30.218	30.508	30.228	29.945	30.150
9	30.312	30.428	29.982	30.328	30.078
10	30.192	30.559	29.882	30.290	30.312
Average value	30.450	30.407	30.123	30.250	30.249
Absolute error	0.418	0.375	0.092	0.218	0.217
Relative error	1.39%	1.12%	0.31%	0.72%	0.72%

five light-pens in TABLE 3, it can be observed that, when the control point dispersion becomes smaller and smaller, the error decreases at first, but begins to increase after the control point dispersion reaches a certain value.

The experimental results show that the dispersion of the light-pen control points does have an impact on the measurement accuracy. The experimental results of the new light-pen with eight control points verified that increasing control point dispersion helps to improve measurement accuracy when the control point dispersion does not exceed a certain range, but overall, the relationship between the control points dispersion and measurement accuracy is not a monotonous increasing trend.

V. CONCLUSION

To study the influence of control point dispersion on measurement accuracy, a light-pen measuring system is developed in this paper. A new type of control point distribution is designed in this system. According to this distribution, five light-pens with different control point dispersions are created, and an algorithm that matches the control points and their images is proposed. The experimental repeatability results indicate that the repeatability of light-pen probe is satisfactory and suitable for experimental research. The experimental measurement results demonstrate that the influence of control point dispersion on measurement accuracy.

The light-pen coordinate measuring system in this paper can meet the requirements of medium measurement accuracy. In future research, we will further increase the measurement accuracy by exploring the influence of other factors.

REFERENCES

[1] D. J. Liu *et al.*, "Parallel mechanism coordinate measuring machine–a new type of high-precision coordinate measuring system," *High-Tech Commun.*, no. 8, pp. 83–85, 2000.
[2] J. Santolaria, D. Guillomía, C. Cajal, J. Albajez, and J. Aguilar, "Modelling and calibration technique of laser triangulation sensors for integration in robot arms and articulated arm coordinate measuring machines," *Sensors*, vol. 9, no. 9, pp. 7374–7396, Sep. 2009, doi: 10.3390/s90907374.
[3] G. Shi and W. Wang, "Single laser complex method to improve the resolution of FMCW laser ranging," *J. Infr. Millim. Waves*, vol. 35, pp. 363–367, 2016.
[4] N. Zhou, Z. Y. An, L. J. Li, and Y. Zhu, "IGPS measurement network multi-station arrangement design," *Appl. Mech. Mater.*, vol. 443, pp. 223–227, Oct. 2013, doi: 10.4028/www.scientific.net/AMM.443.223.
[5] F. Franceschini, D. Maisano, and L. Mastrogiacomo, "Mobile spatial coordinate measuring system (MScMS) and CMMs: A structured comparison," *Int. J. Adv. Manuf. Technol.*, vol. 42, nos. 11–12, pp. 1089–1102, Jun. 2009, doi: 10.1007/s00170-008-1677-0.
[6] X. F. Wang, Z. R. Qiu, C. Yang, Z. Y. Qian, and H. L. Chen, "Calibration method for test sieves based on video measuring machine," *J. Data Acquis. Process.*, vol. 28, no. 2, pp. 257–260, 2013.
[7] M. Company, "Metronor light-pen measuring instrument: Established a new benchmark for portable large-size coordinate measurement systems," *Aeronaut. Manuf. Technol.*, p. 97.
[8] J. Chen, X. Wu, M. Yu, and X. Li, "3D shape modeling using a self-developed hand-held 3D laser scanner and an efficient HT-ICP point cloud registration algorithm," *Opt. Laser Technol.*, vol. 45, pp. 414–423, Feb. 2013, doi: 10.1016/j.optlastec.2012.06.015.
[9] J. Valícek, M. Držík, T. Hryniewicz, M. Harnicárová, K. Rokosz, M. Kucnerová, K. Barcová, and D. Bražina, "Non-contact method for surface roughness measurement after machining," *Meas. Sci. Rev.*, vol. 12, no. 5, pp. 184–188, Jan. 2012.
[10] C. Łukianowicz and T. Karpinski, "Optical system for measurement of surface form and roughness," *Meas. Sci. Rev.*, vol. 1, no. 1, pp. 151–154, 2001. [Online]. Available: https://papers3://publication/uuid/7491C1E7-9F16-473D-907F-7991AAE198CE
[11] Z. X. Xie, Z. W. Zhang, and M. Jin, "Development of a multi-view laser scanning sensor for reverse engineering," *Meas. Sci. Technol.*, vol. 17, no. 8, pp. 2319–2327, 2006.
[12] [Online]. Available: http://www.geodetic.com/v-stars.aspx
[13] Metronor Company Information. [Online]. Available: http://www.hexagonmetronor.com
[14] [Online]. Available: http://www.creaform3d.com/en/metrology-solution/
[15] S. G. Liu, K. Peng, F. S. Huang, and P. Li, "A portable 3D vision coordinate measurement system using a light pen," *Key Eng. Mater.*, vol. 295, pp. 295–296 and 331–336, 2005.
[16] R. Zhang, S. Liu, S. Wang, and X. Song, "Stylus tip center position self-calibration based on invariable distances in light-pen systems," *Sensors*, vol. 17, no. 12, p. 131, Jan. 2017, doi: 10.3390/s17010131.
[17] S. Fu *et al.*, "Light-pen type vision measurement system for on-site measurement of large workpieces," *Chin. J. Sci. Instrum.*, vol. 36, no. 2, pp. 430–438, 2015.
[18] W. Cheng, X. Zhang, and Z. Zhang, "Light pen calibration for a monocular-vision-based coordinate measuring system," in *Proc. 7th Int. Conf. Intell. Hum.-Mach. Syst. Cybern.*, Aug. 2015, pp. 340–344.

[19] W. Li and Y. Li, "Portable monocular light-pen vision measurement system," *J. Opt. Soc. Amer. A, Opt. Image Sci.*, vol. 32, no. 2, pp. 238–247, 2015.
[20] R. Zhang, S. G. Liu, and H. Y. Wang, "Wireless control for pointolite in light-pen CMMs," *Appl. Mech. Mater.*, vol. 602, pp. 2217–2220, 2014.
[21] S. G. Liu, Z. Z. Jiang, Y. H. Dong, and H. L. Zhang, "Sub-regional camera calibration based on moving light target," *Opt. Precis. Eng.*, vol. 22, pp. 259–265, 2014.
[22] G. W. Jiang, "Research on camera chain pose transmission camera measurement method and hull deformation measurement," National Univ. Defense Technol., Changsha, China, Tech. Rep.
[23] X. Weng, "Simulation study of multi-target board pose monocular vision tracking measurement system in a large field of view," Nanjing Univ. Aeronaut. Astronaut., Nanjing, China, Tech. Rep., 2014.
[24] F. S. Huang, "Research on key technology of light-pen single-camera three-dimensional coordinate vision measurement system," 2005, pp. 56–64.
[25] Z. W. Xu and C. K. Wu, "Space plane polygon recognition based on perspective projection invariance," *Chin. J. Electron.*, no. 7, p. 8, 1993.
[26] K. Alblalaihid, P. Kinnell, S. Lawes, D. Desgaches, and R. Leach, "Performance assessment of a new variable stiffness probing system for micro-CMMs," *Sensors*, vol. 16, no. 4, p. 492, Apr. 2016, doi: 10.3390/s16040492.
[27] S. Liu, H. Zhang, Y. Dong, S. Tang, and Z. Jiang, "Portable light pen 3D vision coordinate measuring system-probe tip center calibration," *Meas. Sci. Rev.*, vol. 13, no. 4, pp. 194–199, Aug. 2013, doi: 10.2478/msr-2013-0030.
[28] S. L. Xu and E. N. Ma, *Commonly Used Algorithm for Assembly (C/C++ Language to Describe)*, 3rd ed. Beijing, China: Tsinghua Univ. Press, 2013, pp. 204–210.
[29] F. S. Huang and H. F. Qian, "Light-pen type single camera three-dimensional coordinate vision measurement system," *Photoelectr. Eng.*, vol. 34, no. 4, pp. 69–72, 2007.
[30] J. W. Li *et al.*, "On-site calibration design of SCARA robot weld tracker," *Modular Mach. Tool Autom. Process. Technol.*, no. 5, pp. 2–4, 2017.

DONGRI SHAN received the M.S. degree in mechanical manufacturing and automation from Shandong Industrial University, Jinan, China, in 2000, and the Ph.D. degree in mechanical engineering from Zhejiang University, Hangzhou, in 2003. He is currently a Professor with the School of Electronic and Information Engineering, Qilu University of Technology (Shandong Academy of Sciences), Jinan. His current research interests include intelligent manufacturing and advanced numerical control equipment.

XIAODONG BI received the B.E. degree from the Qilu University of Technology (Shandong Academy of Sciences), Jinan, China, in 2018, where he is currently pursuing the master's degree. His research interests include monocular vision measurement and image processing.

XIAOFANG WANG received the M.S. degree in engineering signal and information processing from the Ocean University of China, Qingdao, in 2005, and the Ph.D. degree in electronic and information from Xi'an Jiaotong University, Xi'an, in 2018. She is currently a Teacher with the Department of Physics, School of Electronic and Information Engineering, Qilu University of Technology (Shandong Academy of Sciences), Jinan, China. Her current research interests include image processing, pattern recognition, and deep learning.

PENG ZHANG received the B.S. and M.S. degrees from the Qilu University of Technology (Shandong Academy of Sciences), China, in 2000 and 2003, respectively, and the Ph.D. degree in detection technology and automation from Tongji University, China, in 2010. He is currently an Associate Professor with the Qilu University of Technology (Shandong Academy of Sciences). His research interests include intelligent detection and control technology, robotics, and numerical control technology.

ZHOUFANG XU received the master's degree in microelectronics and solid-state electronics from Shandong Normal University, in 2010, and the Ph.D. degree in communication and information system from Shandong University, in 2014. She is currently a Lecturer with the Qilu University of Technology (Shandong Academy of Sciences), Jinan, China. Her research interests include brain–computer interface and pattern recognition.

MIN HAN received the M.S. degree in science and the Doctor of Engineering degree from the Beijing Institute of Technology, in 2010 and 2016, respectively. Since 2016, she has been working with the Qilu University of Technology (Shandong Academy of Sciences). She is mainly engaged in the exploratory research of graphene as beam splitter, various passive devices of graphene material: waveguide, passive/active filter, transmission line, power divider, and coupler.

YANG LIU received the B.S. degree from the China University of Geosciences, in 2013, and the Ph.D. degree from Jilin University, China, in 2020. After his Ph.D., he joined Jilin University, where he is carrying out research and working on stereo vision, 3-D reconstruction, and image segmentation.

CHENGLONG ZHANG received the B.E. degree from the Qilu University of Technology (Shandong Academy of Sciences), Jinan, China, in 2019, where he is currently pursuing the master's degree. His research interests include monocular vision measurement and image processing.

YALU XU received the B.E. degree from the Taiyuan University of Technology of China, Taiyuan, China, in 2019. He is currently pursuing the master's degree with the Qilu University of Technology (Shandong Academy of Sciences), China. His research interests include deep learning and object detection.